

Customizable Reference Runtime Monitoring of Neural Networks using Resolution Boxes^{*}

Changshun Wu¹, Yliès Falcone², and Saddek Bensalem¹

¹ Univ. Grenoble Alpes, CNRS, Grenoble INP, Verimag, 38000 Grenoble, France

² Univ. Grenoble Alpes, Inria, CNRS, Grenoble INP, LIG, 38000 Grenoble, France

Abstract. Classification neural networks fail to detect inputs that do not fall inside the classes they have been trained for. Runtime monitoring techniques on the neuron activation pattern can be used to detect such inputs. We present an approach for the runtime verification of classification systems via data abstraction. Data abstraction relies on the notion of box with a resolution. Box-based abstraction consists in representing a set of values by its minimal and maximal values in each dimension. We augment boxes with a notion of resolution; this allows to define the notion of clustering coverage, which is intuitively a quantitative metric over boxes that indicates the quality of the abstraction. This allows studying the effect of different clustering parameters on the constructed boxes and estimating an interval of sub-optimal parameters. Moreover, we show how to automatically construct monitors that make use of both the correct and incorrect behaviors of a classification system. This allows checking the size of the monitor abstractions and analysing the separability of the network. Monitors are obtained by combining the sub-monitors of each class of the system placed at some selected layers. Our experiments demonstrate the effectiveness of our clustering coverage estimation and show how to assess the effectiveness and precision of monitors according to the selected clustering parameter and the chosen monitored layers.

1 Introduction

During the past decade, the growth of computing power and the abundance of data from all kinds of sources have changed many fields of science and technology, from biology and medicine to economy and social sciences. The so-called (new) artificial intelligence (AI)³ revolution is also reshaping our entire industry, our society, and our day-to-day lives. In fact, it is quite reasonable to say that after a long “winter sleep”, AI is once again flourishing thanks to recent advances in machine learning (ML) algorithms. Today, many systems already incorporate an increasing amount of intelligence and autonomy (face recognition, industrial robotics, data processing, etc.). More specifically, the AI System technologies are expected to bring large-scale improvements through new products and services across a myriad of applications ranging from healthcare to logistics through manufacturing, transport and more.

Today’s AI-based systems rely on so-called learning-enabled components (LECs) [35]. For example, a learning-enabled autonomous system may rely on a LEC performing visual perception and recognition. To trust the AI system we must also trust its LECs. However, such systems (especially deep recurring neural networks) are highly unpredictable [44]. Prototyping such systems may seem quick and easy, but prototypes are not safe and incur a high cost, referred to as technical debt [41]. These problems are not theoretical. Traffic violations, accidents, and even human casualties have resulted from faults of LECs. It

^{*} This paper is supported by the European Union’s Horizon 2020 research and innovation programme under grant agreement No. 956123 - FOCETA and the French national program “Programme Investissements d’Avenir IRT Nanoelec” (ANR-10-AIRT-05).

³ AI is used in a broad sense, to include many related fields and buzzwords, such as machine learning, big data, data science, and so on.

is therefore correctly and widely recognized that AI-based systems are not often trustworthy [22]. The safety-critical nature of such systems involving LECs raises the need for formal methods [42]. In particular, how do we systematically find bugs in such systems? We believe that we need formal verification techniques, in order to i) model AI systems, and in particular their LECs; ii) specify what properties these systems have, or should have; iii) reason about such properties and ultimately verify that they are satisfied. Indeed, these research areas are currently emerging, see for instance [21].

Unfortunately, traditional verification techniques are not usable for such purpose for several reasons. First, LECs are generally not specified; they are essentially obtained from examples and the explainability of their synthesis and implementation is not well understood. Second, such components take as input complex data, typically highly dimensional vectors with immense state space. Third, the abnormal behaviors are often discovered when the system is in operation. Some of the essential properties of such systems cannot be guaranteed statically at design time. These properties should be enforced at runtime by using monitoring and control-based techniques.

Verification techniques for data-driven learning components have been actively developed in the past 3-4 years [9,10,12,24,31,34,37,39,47,28]. However, their scalability is required to be significantly improved to meet industrial needs. Safety-critical systems involving LECs like self-driving cars, extensively use data-based techniques, for which we do not have so far a theory allowing behavioural predictability. To favor scalability, some research efforts in the last few years have focused on using dynamic verification techniques such as testing [36,43,46,48,50] and runtime verification [6,19,32,5].

In this paper, we contribute to the research efforts on runtime verification for learning-enabled components. In designing a runtime verification approach for learning-enabled components, one of the main challenges is the absence of a clear behavioral specification of the component to be checked at runtime. This implies a fundamental shift in the paradigm: to move from behavior-based verification to data-based verification. Henceforth, existing approaches essentially proceed in two steps. First, one characterizes the seen data (e.g., via probability distribution) or the compact patterns generated from them (via Boolean or high-dimension geometry abstraction). Then, one uses the established characterizations as references to check the system decisions on new inputs by checking the similarity between the produced patterns at runtime and the reference patterns. The above pioneering approaches can be split in two categories depending on the abstractions used to record the reference patterns: Boolean abstraction [6,5] and geometrical-shape abstraction [19,32,5].

Approach and contributions. We focus on the monitoring approaches based on geometrical shape abstraction. In particular, we extend the work in [19] to address some of its limitations. The approach in [19] only leverages the good reference behavior of the network. Ignoring bad reference behavior discards some useful information. The geometrical shape abstractions of the good and bad reference behaviour may intersect or not. Thus, a new generated pattern can belong to both abstractions. Hence, the verdicts produced by [19] based only on behaviors may be partial. We use both the good and bad network behaviours correct and incorrect decisions respectively) as references to build box abstractions. Using these references, at an abstract level, a runtime monitor assigns verdicts to a new input as follows:

- if the input generates patterns (e.g., output values at close-to-output layers) that fall only within the good references, then the input is accepted;
- if the input generates patterns captured by both the good and bad references, it marks the input as uncertain;

– otherwise, the input is rejected.

Introducing uncertainty verdicts allows identifying suspicious regions when the abstractions of good and bad references overlap. By reducing the abstraction size, one may remove the overlapping regions and obtain suitable abstraction size. Otherwise, it indicates that the network does not have a good separability: the positive and negative samples are tangled. This provides feedback to the network designer. It also permits comparing the regions of patterns and thus enables the study of the relationship between good and bad behavior patterns of the network. Moreover, we introduce the notion of *box with resolution* which consists intuitively in tiling the space of a box. By doing this, one can measure the clustering coverage which is an indicator of the coarseness of the abstraction. Using the clustering coverage, we can assess the precision of the boxes. In choosing the box resolution, there is a tradeoff between the precision of the related abstractions and the related overhead (i.e., augmenting the precision augments the overhead). To control the precision, we discuss how to tune the clustering parameters by observing the clustering coverage and the number of uncertainties. We achieve better precision and recall in all cases.

Paper organization. The rest of this paper is structured as follows. Section 2 introduces preliminary concepts and notation. Section 3 defines boxes with a resolution. Section 4 presents our monitoring framework. Section 5 presents the results of our experimental evaluations. Section 6 positions our work and details the improvements over state-of-the-art approaches. Section 7 concludes.

2 Preliminaries

For a set E , $|E|$ denotes the cardinality of E . Let \mathbb{N} and \mathbb{R} be the sets of natural and real numbers, respectively. For $x \in \mathbb{R}$, $\lceil x \rceil$ denotes the ceiling of x , that is the least integer greater than x . To refer to intervals of integers, we use $[a \cdots b]$ with $a, b \in \mathbb{N}$ and $a \leq b$. To refer to intervals of real numbers, we use $[a, b]$ with $a, b \in \mathbb{R} \cup \{-\infty, \infty\}$ and if $a, b \in \mathbb{R}$, then $a \leq b$. For $n \in \mathbb{N} \setminus \{0\}$, $\mathbb{R}^n \stackrel{\text{def}}{=} \underbrace{\mathbb{R} \times \cdots \times \mathbb{R}}_{n \text{ times}}$ is the space of real coordinates of dimension n and its elements are called n -dimensional vectors. We use $\mathbf{x} = (x_1, \dots, x_n)$ to denote an n -dimensional vector and $\theta_i : \mathbb{R}^n \rightarrow \mathbb{R}$ the projection function on the i -th dimension for $i \in [1 \cdots n]$, i.e., $\theta_i(\mathbf{x}) = x_i$.

2.1 Feedforward Neural Networks

A neuron is an elementary unit mathematical function. A (*forward*) *neural network* (NN) is a sequential structure of $L \in \mathbb{N} \setminus \{0\}$ layers, where, for $i \in [1 \cdots L]$, the i -th layer comprises d_i neurons and implements a function $g^{(i)} : \mathbb{R}^{d_{i-1}} \rightarrow \mathbb{R}^{d_i}$. In a network, the inputs of neurons at layer i comprise (1) the outputs of neurons at layer $(i - 1)$ and (2) a bias. Moreover, the outputs of neurons at layer i are inputs for neurons at layer $i + 1$.

Given a network input $\mathbf{x} \in \mathbb{R}^{d_0}$, the output at the i -th layer is computed by the function composition $f^{(i)}(\mathbf{x}) \stackrel{\text{def}}{=} g^{(i)}(\cdots g^{(2)}(g^{(1)}(\mathbf{x})))$. For networks used for classification tasks, aka classification networks, the *decision* $\text{dec}(\mathbf{x})$ of classifying input \mathbf{x} into a certain class is given by the index of the neuron of the output layer whose value is maximum, i.e., $\text{dec}(\mathbf{x}) \stackrel{\text{def}}{=} \text{argmax}_{1 \leq i \leq d_L} \theta_i(f^{(L)}(\mathbf{x}))$. In this paper, we only consider well-trained networks, i.e., networks in which the weights and bias related to neurons are fixed. The method developed in what follows is applicable to networks with various neuron activation functions.

2.2 Abstraction for Neural Networks

To construct runtime monitors, we need to use and represent the high-level features from NNs, which are large sets of vectors. For this, the classical approach in verification is to use *abstraction* techniques (e.g., abstract interpretation [7]) to over-approximate a given set of finite vectors into a set of mathematical constraints. Abstraction techniques have recently also been used for NNs, e.g., *abstract interpretation* and *intervals bound* are used to verify the network’s safety and robustness [12,14], along with *boolean* [6] and *box* [19] abstraction for runtime monitoring of NNs.

As runtime monitoring of NNs require intensive usage of the high-level features, affordable computational complexity of *storage*, *construction*, *membership query*, and *coarseness control* is paramount. While there are other candidate abstractions using different geometry shapes (such as *zonotope*, and *polyhedra*), our preliminary study of these alternative shapes along with the complexity considerations, led to choose to follow [19] and use box abstraction for the purpose of this paper.

2.3 Box Abstraction [19]

We briefly review box abstraction. A box is essentially a set of contiguous n -dimensional vectors constrained by real intervals.

Definition 1 ((tight) Box abstraction). For a set $X \subseteq \mathbb{R}^n$ of n -dimensional vectors, its (tight) box abstraction is defined as $B(X) \stackrel{\text{def}}{=} \left\{ (x_1, \dots, x_n) \in \mathbb{R}^n \mid \bigwedge_{i \in [1..n]} a_i \leq x_i \leq b_i \right\}$, where $a_i = \min(\{\theta_i(\mathbf{x})\})$ and $b_i = \max(\{\theta_i(\mathbf{x})\})$, for $\mathbf{x} \in X$ and $i \in [1 \dots n]$.

The box is said to be tight because the interval built on each dimension is the minimum one containing all the values of the given points on the corresponding dimension. We only consider tight boxes and refer to them as boxes.

A box is equivalently encoded as the list of intervals of its bounds on each dimension, i.e., and we equivalently note $B(X) = [[a_1, b_1], \dots, [a_n, b_n]]$. Moreover, given two n -dimensional boxes $B(X') = [[a'_1, b'_1], \dots, [a'_n, b'_n]]$ and $B(X) = [[a_1, b_1], \dots, [a_n, b_n]]$, $B(X')$ is said to be a *sub-box* of $B(X)$ if the vectors of $B(X')$ are all in $B(X)$, i.e., if $\forall i \in [1 \dots n] : a_i \leq a'_i \wedge b'_i \leq b_i$. For two datasets X' and X , if $X' \subseteq X$, then $B(X')$ is a sub-box of $B(X)$. Furthermore, the *emptiness check* of a box as well as the *intersection* between two n -dimensional boxes is a box and can be easily computed using their lower and upper bounds on each dimension.

Example 1 ((tight) Box abstraction). Considering a set of vectors (dataset) $X = \{(0.1, 0.5), (0.1, 1.0), (0.2, 0.8), (0.6, 0.2), (1.0, 0.3)\}$, its box abstraction $B(X)$ is the set

$$\left\{ (x_1, x_2) \in \mathbb{R}^2 \mid x_1 \in [0.1, 1.0], x_2 \in [0.2, 1.0] \right\},$$

which can be encoded as $[[0.1, 1.0], [0.2, 1.0]]$.

Remark 1. A box abstracting a set of n -dimensional vectors can be represented by $2 \times n$ bounds. The complexity of building a box for a set of n -dimensional vectors of cardinal m is $O(m \times n)$, while the membership query of a vector in a box is $O(n)$. The control of the coarseness or size of a box can be easily realized by enlarging or reducing the bounds.

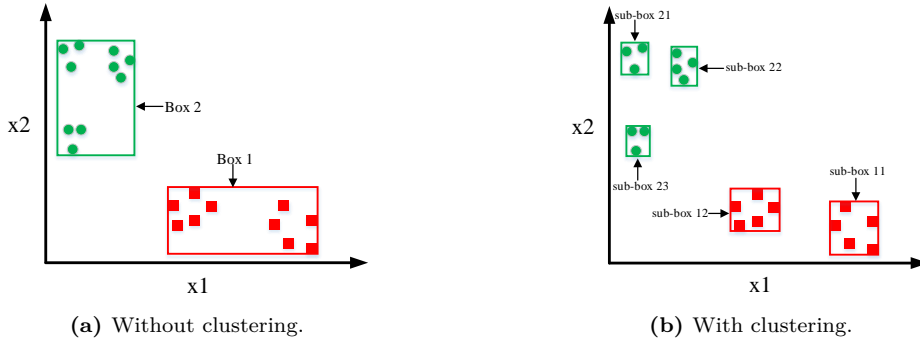


Fig. 1: Box abstractions for two sets of points (the green and red one) built without and with clustering.

2.4 Clustering

In certain cases, the box abstraction of a set X is such that most of the elements of X end up close to the boundaries of the box (there is “white space”). For instance, this is the case with the two boxes in Fig. 1a. Consequently, more elements not originally present in the set end up in the box abstraction. This situation is not desirable for our monitoring purpose.

To remedy this, one can apply a clustering algorithm to determine a partition of the set based on an appropriate similarity measure such as distance (e.g., k -means clustering [30]), density (DBSCAN [40]), connectivity (hierarchical clustering [33]), etc. Finding the best clustering algorithms for monitoring remains an open question out of the scope of this paper. We choose to adopt k -means even though other clustering algorithms are certainly also usable with our monitoring framework.

By grouping the points that are close to each other in a cluster and computing the box abstractions on each cluster separately, abstracting these sets more precisely as the union of the boxes computed for each cluster. Consequently, by using clustering first and then abstraction, we end up with a set of boxes based on the partitions determined by the clustering algorithms. Clustering and its benefit in terms of precision are illustrated in Fig. 1b.

3 Boxes with a Resolution

Applying a clustering algorithm before computing abstractions for a set of points was first proposed in [19]. Clustering is essential to construct the monitor therein. The clustering parameters directly influence the monitor performance. However, the effect of using clustering algorithms in monitoring nor the relationship between the clustering parameters and the monitor performance were not discussed and studied in [19]. Moreover, going back to Fig. 1, with boxes, we observe that it is difficult to *quantify* the precision of the abstraction provided by boxes.

To address the aforementioned problems, we introduce the notion of *box with a resolution* providing insights into the relationship between the clustering parameters and the performance of the monitor. Specifically, a box with a resolution computed for a set of points is a box divided into a certain number of cells of the same size. Moreover, the ratio between the number of cells covered by the set of boxes computed for the partition of the set of points (obtained by clustering) to the total number of cells can be used to measure the relative coarseness of the box abstractions computed with and without clustering. We

refer to this metric as the *clustering coverage*. The purpose of this section is to compute efficiently (an approximation) of the clustering coverage using box abstraction.

In the following, we consider a set X of n -dimensional vectors, its n -dimensional box (abstraction) $B(X) = [[a_1, b_1], \dots, [a_n, b_n]]$, its *partition* $\pi(X) = \{X^1, \dots, X^k\}$ obtained by a clustering algorithm, and the set of boxes computed for the partitioned dataset $\mathcal{B}_X = \{B^1, \dots, B^k\}$ where $B^i = B(X^i)$ for $i \in [1 \dots k]$. We refer informally to $B(X)$ as the global box and to B^1, \dots, B^k as the local boxes. Our goal is to measure the relative sizes of the local boxes to the global one. When computing the local boxes, we observe that they often exist on different dimensions, i.e., some of their intervals is of length 0.

Box covered space. We start by introducing the notion of *box covered space*. Intuitively, the box covered space associated with $B(X)$ is a box of (possibly) lower dimension used for measuring the spaced covered.

Definition 2 (Box covered space). *The covered space of $B(X)$ is defined as $CovB(X) \stackrel{\text{def}}{=} [[a_i, b_i] \text{ if } a_i \neq b_i \mid [a_i, b_i] \in B(X)]$.*

That is, the covered space of $B(X)$ is the box encoded as the list of non-zero-length intervals of $B(X)$.

Example 2 (Box covered space). Consider dataset $X = \{(1.5, 2.0, 1), (1.8, 2.3, 1)\}$ and its box $B(X) = [[1.5, 1.8], [2.0, 2.3], [1, 1]]$. Its box covered space is $CovB(X) = [[1.5, 1.8], [2.0, 2.3]]$.

Adding resolution. Let $|CovB(X)|$ denote the length of $CovB(X)$ – it is the number of dimensions on which the box abstraction of X exists. We divide each interval/dimension of $CovB(X)$ into $|X|$ subintervals of the same length. Consequently, the space enclosed in $CovB(X)$ is equally divided into $|X|^{|CovB(X)|}$ subspaces. Each such a subspace is called a *box cell*. Each box cell can be encoded (as a box) by $|CovB(X)|$ intervals and can be indexed by coordinates of size $|CovB(X)|$. We can hence reuse the notions and notations related to boxes. We use \mathcal{C}_X to denote the set of cells obtained from $CovB(X)$.

Definition 3 (Covered cells). *A box cell $c \in \mathcal{C}_X$ is said to be covered by a box $b \in \mathcal{B}_X$ if $c \cap b \neq \emptyset$. The set of covered cells by a box b , $\{c \in \mathcal{C}_X \mid c \cap b \neq \emptyset\}$, is denoted by $CovCell(b)$.*

Using the intervals defining a local box b and the global box $B(X)$, we can compute the number of covered cells in $b \in \mathcal{B}$.

Property 1 (Number of covered cells). For $b \in \mathcal{B}$, let $b = [[a'_1, b'_1], \dots, [a'_n, b'_n]]$, we have: $|CovCell(b)| = \prod_{i=1}^n n_i$, with:

$$n_i = \begin{cases} \left\lceil \frac{|X| \times (a'_i - a_i)}{(b_i - a_i)} \right\rceil - \left\lceil \frac{|X| \times (b'_i - a_i)}{(b_i - a_i)} \right\rceil + 1 & \text{if } b'_i \neq a'_i, \\ 1 & \text{otherwise.} \end{cases}$$

With the number of covered cells, we can define the coverage of a sub-box to a (larger) box.

Definition 4 (Sub-box coverage). *The sub-box coverage of $b \in \mathcal{B}_X$ to $B(X)$ is defined as: $\text{coverage}_X(b) = \frac{|CovCell(b)|}{|X|^{|CovB(X)|}$.*

The sub-box coverage of b to $B(X)$ is the ratio of the number of cells covered by b to the total number of cells in $CovB(X)$.

Example 3 (Sub-box coverage). Considering the set X in Example 1 and its subset $X^1 = \{(0.1, 0.5), (0.1, 1.0), (0.2, 0.8)\}$ along with the corresponding covered space $CovB(X) = [[0.1, 1.0], [0.2, 1.0]]$, the coverage of sub-box $B(X^1) = [[0.1, 0.2], [0.5, 1.0]]$ is:

$$coverage_X(B(X^1)) = \frac{|CovCell(B(X^1))|}{|X|^2} = 4/25.$$

Clustering coverage estimation. We extend the notion of sub-box coverage to set \mathcal{B}_X of local boxes. We note it $coverage_X(\mathcal{B}_X)$ and define it as the ratio between the total number of cells covered by the union of boxes in \mathcal{B}_X to the whole number of cells in $CovB(X)$: $coverage_X(\mathcal{B}_X) = coverage_X(\cup_{b \in \mathcal{B}_X} b)$.

The exact value of $coverage_X(\mathcal{B}_X)$ can, in theory, be easily computed. However, in practice the computation may be very expensive with high dimensionality due to the large number of cells and intersections between boxes.

Henceforth, we only estimate the coverage value by only considering the pair-wise intersections of boxes. This is a reasonable approximation because the set of sub-boxes considered is built from a partition of the input dataset after applying a clustering algorithm: in principle a good clustering implies few elements in the intersections between the clusters, especially if the number of clusters is important.

For \mathcal{B}_X , we define $\mathcal{B}_X^{int} = \{b_i \cap b_j \mid i \in [1 \dots k - 1], j \in [i + 1 \dots k]\}$ as the set of pair-wise intersections of boxes in \mathcal{B}_X .

Proposition 1 (Clustering coverage estimation). *The clustering coverage is lower and upper bounded by r_l and r_u , respectively, where:*

$$r_u = \sum_{b \in \mathcal{B}_X} coverage_X(b) \text{ and } r_l = r_u - \sum_{b \in \mathcal{B}_X^{int}} coverage_X(b).$$

Example 4 (Clustering coverage). Considering the set X in Example 1, we assume that it is partitioned into two clusters $X^1 = \{(0.1, 0.5), (0.1, 1.0), (0.2, 0.8)\}$ and $X^2 = \{(0.6, 0.2), (1.0, 0.3)\}$ along with two smaller boxes $B(X^1) = [[0.1, 0.2], [0.5, 1.0]]$ and $B(X^2) = [[0.6, 1.0], [0.2, 0.3]]$, then the clustering coverage is 0.28 because:

$$r_l = r_u = \frac{|CovCell(B(X^1))| + |CovCell(B(X^2))|}{5^2} = \frac{4 + 3}{25} = 0.28.$$

Remark 2. The clustering coverage allows to better assess the amount of “blank space” between the points in a given set. The lower the value is, the more blank space there exists. On the one hand, obtaining smaller clusters (equivalence classes) before applying abstraction technique augments the precision of the abstraction. On the other hand, having too small clusters has drawbacks: (1) it augments the computational overhead, and (2) it induces some form of overfitting for the monitor. We further demonstrate the effect of clustering in our experiments.

4 Runtime Monitoring of NNs using Resolution Boxes

The frameworks defined in [6,19] *only* utilize the high-level features obtained from the layers close to the output layer (aka, close-to-output layers). Moreover, to build the monitor, [6,19] *only* consider “good behaviors”, i.e., the features of correctly classified inputs

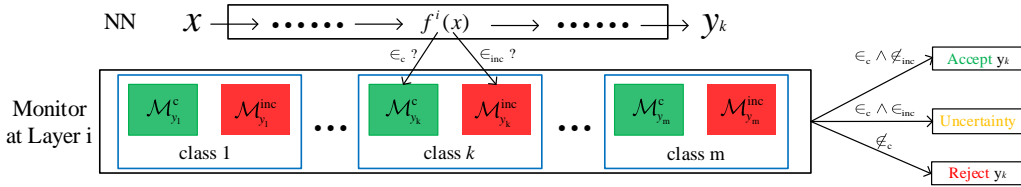


Fig. 2: Framework of runtime monitoring of neural networks.

as reference. Our framework inspires from [6,19] but additionally makes use of the “bad behaviors”, i.e. the ones of misclassified inputs. This has two advantages. First, it allows refining the monitor output by adding a notion of *uncertainty* to the previous monitor verdicts, i.e., *accept* and *reject*. Second, when the monitor produces “uncertainty” as output, it avoids false negatives.

4.1 Clustering Parameter Selection using Resolution

In this subsection, using the clustering coverage estimation from the previous section, we show how we can adjust the clustering parameter of the k -means clustering algorithm. Recall that the k -means algorithm divides a set of N samples from a set X into k disjoint clusters $C = \{C^1, \dots, C^k\}$ [30]. Each cluster C_j is represented by the mean μ_j of the samples in the cluster. The *clustering parameter* τ serves as a threshold for determining the number k of clusters as follows. Essentially, the algorithm starts by grouping the inputs into one cluster and iteratively increment the number of cluster. At each step it computes the so called inertia, where at step k , $inertia^k = \sum_{j=1}^k \sum_{i=1}^{|C^j|} \|x_i - \mu_j\|^2$ and computes the improvement over the previous step and compares it to the threshold τ . That is, it checks whether $1 - \frac{inertia^{k+1}}{inertia^k} < \tau$ and stops if the answer is positive⁴.

In the following, for a given set of n -dimensional vectors V , let $\pi_\tau(V)$ denote the partition of V by using τ for the k -means clustering algorithm and $\overline{coverage_X}(\pi_\tau(V))$ be the mean value of the estimated bounds of clustering coverage using the method from Sec. 3.

Our experiments suggested (see Sec. 5.1) that the difference of clustering coverage between the parameters τ in the regions close to two endpoints is very small, that is the higher variations of clustering coverage with τ mainly happen in an intermediate interval of $[0, 1]$. Thus, it is of interest to identify such regions by determining the maximum value τ_{\max} (resp. the minimum τ_{\min}) whose corresponding clustering coverage is close enough to the one for which $\tau = 1$ (resp. $\tau = 0$). For identifying such regions, we use binary searches of the values of τ_{\min} and τ_{\max} with two user-specified thresholds: ϵ_{cov} for coverage difference and ϵ_{ival} for interval length. Since searching procedures for τ_{\min} and τ_{\max} are similar, we only present the one for τ_{\max} in Algorithm 1. The search starts from boundaries of interval $[0, 1]$ (line 1) and iterate to update one of τ_{\min_u} and τ_{\max_u} by its mean τ_{mean} as follows (line 4 – 7): if $\overline{coverage_X}(\pi_1(V)) - \overline{coverage_X}(\pi_{\tau_{\text{mean}}}(V)) > \epsilon_{\text{cov}}$, $\tau_{\min_u} = \tau_{\text{mean}}$; otherwise $\tau_{\max_u} = \tau_{\text{mean}}$. The iteration will stop until the length of interval $[\tau_{\min_u}, \tau_{\max_u}]$ is lesser than or equal to ϵ_{ival} . The other algorithm for τ_{\min} can be similarly realized by

⁴ In practice, for a given τ , searching the fine number of clusters from $k = 1$ may lead to waste of computational resource. To avoid this, one can store the results of fine number of clusters for the tried values of clustering parameter into a dictionary. When a new τ is input, one can start the search from the fine number of clusters corresponding to the least existing value of clustering parameter less than the new input τ . If all existing values of τ are less than the new one, one starts the search from $k = 1$.

replacing the condition in line 4 by $\overline{coverage_X(\pi_{\tau_{\text{mean}}}(V))} - \overline{coverage_X(\pi_0(V))} > \epsilon_{\text{cov}}$, inverting instructions 5 and 7, and returning τ_{min} .

Then, one can roughly divide the domain of τ into three parts: $[0, \tau_{\text{min}}]$, $[\tau_{\text{min}}, \tau_{\text{max}}]$, and $[\tau_{\text{max}}, 1]$. Each part demonstrates the correlated effect on partitioning the dataset in terms of space coverage. Based on this, one can fine-tune the value of τ according to the monitor performance (see Sec. 5.2). We believe that this can also be used with other geometrical shape abstractions for initial clustering parameter selection, especially when the enclosed space is hard to calculate in high-dimensional space, e.g., zonotope and polyhedra.

Algorithm 1 Search of clustering parameter τ_{max}

Input: V (a set of n -dimensional vectors), ϵ_{cov} (threshold of coverage difference), ϵ_{ival} (threshold of interval length)

Output: clustering parameter τ_{max}

```

1:  $\tau_{\text{min}_u}, \tau_{\text{max}_u} \leftarrow 0, 1$ 
2: while  $\tau_{\text{max}_u} - \tau_{\text{min}_u} > \epsilon_{\text{ival}}$  do
3:    $\tau_{\text{mean}} = (\tau_{\text{max}_u} + \tau_{\text{min}_u})/2$ ;
4:   if  $\overline{coverage_X(\pi_1(V))} - \overline{coverage_X(\pi_{\tau_{\text{mean}}}(V))} > \epsilon_{\text{cov}}$  then
5:      $\tau_{\text{min}_u} = \tau_{\text{mean}}$ 
6:   else
7:      $\tau_{\text{max}_u} = \tau_{\text{mean}}$ 
8:   end if
9: end while
10: return  $\tau_{\text{max}_u}$ 

```

4.2 Monitor Construction

We construct monitors and attach them to some specific chosen layers. For a given layer ℓ and each output class $y \in \mathcal{Y}$, we construct a monitor $\mathcal{M}_{y,\ell}$. A monitor comprises two parts, $\mathcal{M}_{y,\ell}^c$ and $\mathcal{M}_{y,\ell}^{\text{inc}}$, both of which are sets of abstractions used as references of high-level features for inputs correctly and incorrectly classified as y , respectively.

Algorithm 2 constructs the monitor in three steps: i) extract the values of high-level features at monitored layer ℓ (line 1 and 2); ii) apply clustering algorithm to the obtained features and partition them into local distributed clusters (line 3), see Sec. 4.1; iii) construct an abstraction for each cluster. The union of abstractions computed as such forms $\mathcal{M}_{y,\ell}^c$.

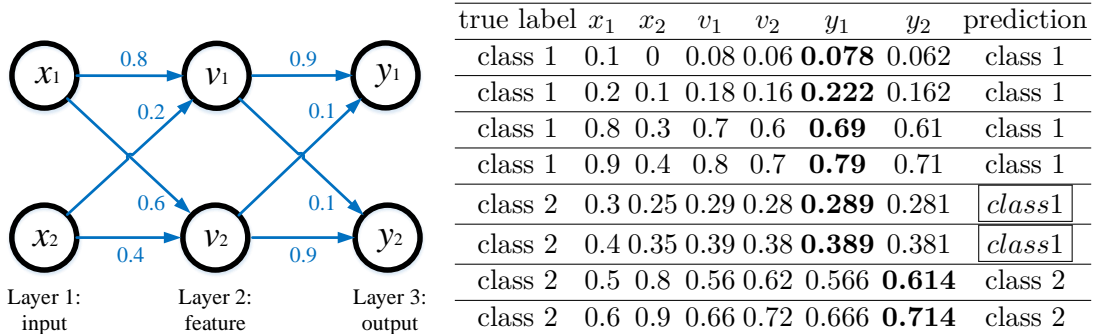


Fig. 3: An example of neural network. **Table 1:** Data and patterns related to the network in Fig. 3.

Below is an example for illustrating the algorithm above.

Example 5. Consider the network in Fig. 3 and the data used to build its monitor are given by columns 1-3 in Table 1. We consider output class 1 at layer 2. Algorithm 2:

Algorithm 2 Construct abstraction for class y at layer ℓ

Input: $y \in \mathcal{Y}$ (output class), ℓ (monitored layer), $D = \{(\mathbf{x}^1, y^1), \dots, (\mathbf{x}^m, y^m)\}$ (training data), τ (clustering parameter)

Output: $\mathcal{M}_{y,\ell} = (\mathcal{M}_{y,\ell}^c, \mathcal{M}_{y,\ell}^{\text{inc}})$ (a pair of two sets of abstractions)

- 1: $V_{y,\ell}^c \leftarrow \{f^\ell(\mathbf{x}) \mid (\mathbf{x}, y') \in D \wedge y' = y \wedge y = \mathbf{dec}(\mathbf{x})\}$
(* collect the neuron values at layer ℓ for inputs correctly classified in y *)
 - 2: $V_{y,\ell}^{\text{inc}} \leftarrow \{f^\ell(\mathbf{x}) \mid (\mathbf{x}, y') \in D \wedge y' \neq y \wedge y = \mathbf{dec}(\mathbf{x})\}$
(* collect the neuron values at layer ℓ for inputs incorrectly classified as class y *)
 - 3: $\mathbb{C}_{y,\ell}^c, \mathbb{C}_{y,\ell}^{\text{inc}} \leftarrow \mathbf{cluster}(V_{y,\ell}^c, \tau), \mathbf{cluster}(V_{y,\ell}^{\text{inc}}, \tau)$ (* divide collected vectors into clusters *)
 - 4: $\mathcal{M}_{y,\ell}^c, \mathcal{M}_{y,\ell}^{\text{inc}} \leftarrow \emptyset, \emptyset$ (* sets of abstractions for class y *)
 - 5: **for** $C \in \mathbb{C}_{y,\ell}^c, C' \in \mathbb{C}_{y,\ell}^{\text{inc}}$ **do**
 - 6: $A_{y,\ell}^C, A_{y,\ell}^{C'} \leftarrow \mathbf{abstract}(C), \mathbf{abstract}(C')$
(* construct abstractions for vectors in cluster C and C' *)
 - 7: $\mathcal{M}_{y,\ell}^c, \mathcal{M}_{y,\ell}^{\text{inc}} \leftarrow \mathcal{M}_{y,\ell}^c \cup \{A_{y,\ell}^C\}, \mathcal{M}_{y,\ell}^{\text{inc}} \cup \{A_{y,\ell}^{C'}\}$
 - 8: **end for**
 - 9: **return** $\mathcal{M}_{y,\ell} = (\mathcal{M}_{y,\ell}^c, \mathcal{M}_{y,\ell}^{\text{inc}})$
-

1. extracts the features (values of v_1 and v_2 in Table 1) generated at layer 2 and classify them into two sets $V_{1,2}^c = \{(0.078, 0.062), (0.222, 0.162), (0.69, 0.61), (0.79, 0.71)\}$ and $V_{1,2}^{\text{inc}} = \{(0.289, 0.281), (0.389, 0.381)\}$ according to whether their inputs are correctly classified or not.
2. partitions set $V_{1,2}^c$ into a set of two clusters $\mathbb{C}_{1,2}^c = \{C_1, C_2\}$ with:
 - $C_1 = \{(0.078, 0.062), (0.222, 0.162)\}$,
 - $C_2 = \{(0.69, 0.61), (0.79, 0.71)\}$,and keep $V_{1,2}^{\text{inc}}$ as a single cluster $\mathbb{C}_{1,2}^{\text{inc}} = \{C_3\}$ with $C_3 = \{(0.289, 0.281), (0.389, 0.381)\}$;
3. builds the box abstractions for each cluster obtained at step 2: $A_{1,2}^{C_1} = B(C_1) = [[0.078, 0.222], [0.062, 0.162]]$, $A_{1,2}^{C_2} = B(C_2) = [[0.69, 0.79], [0.61, 0.71]]$, and $A_{1,2}^{C_3} = B(C_3) = [[0.289, 0.389], [0.281, 0.381]]$.

The monitor for class 1 is the pair of sets: $\mathcal{M}_{1,2} = (\mathcal{M}_{1,2}^c, \mathcal{M}_{1,2}^{\text{inc}})$, where $\mathcal{M}_{1,2}^c = \{A_{1,2}^{C_1}, A_{1,2}^{C_2}\}$ and $\mathcal{M}_{1,2}^{\text{inc}} = \{A_{1,2}^{C_3}\}$.

4.3 Monitor Execution

Algorithm 3 Monitoring at Layer ℓ

Input: network input \mathbf{x} , pairs of two sets of abstractions: $\mathcal{M}_{1,\ell} = (\mathcal{M}_{1,\ell}^c, \mathcal{M}_{1,\ell}^{\text{inc}}), \dots, \mathcal{M}_{|\mathcal{Y}|,\ell} = (\mathcal{M}_{|\mathcal{Y}|,\ell}^c, \mathcal{M}_{|\mathcal{Y}|,\ell}^{\text{inc}})$

Output: answer “accept”, “reject”, or “uncertainty”

- 1: $S_correct, S_incorrect \leftarrow False, False$
(* flags used to record if the new produced output is similar to correct or incorrect behavior *)
 - 2: $\mathbf{v} \leftarrow f^\ell(\mathbf{x})$ (* collect output at layer ℓ *)
 - 3: $y \leftarrow \mathbf{dec}(\mathbf{x})$ (* predict class of \mathbf{x} *)
 - 4: **if** $\mathbf{v} \in \mathcal{M}_{y,\ell}^c$ **then**
 - 5: $S_correct \leftarrow True$ (* found a correct-classification abstraction containing \mathbf{v} *)
 - 6: **end if**
 - 7: **if** $\mathbf{v} \in \mathcal{M}_{y,\ell}^{\text{inc}}$ **then**
 - 8: $S_incorrect \leftarrow True$ (* found an incorrect-classification abstraction containing \mathbf{v} *)
 - 9: **end if**
 - 10: **if** $S_correct \wedge S_incorrect$ **then**
 - 11: **return** “uncertainty” (* \mathbf{v} is contained by both \mathcal{M}_y^c and $\mathcal{M}_y^{\text{inc}}$ *)
 - 12: **else if** $S_correct \wedge \neg S_incorrect$ **then**
 - 13: **return** “accept” (* \mathbf{v} is only contained by \mathcal{M}_y^c *)
 - 14: **else**
 - 15: **return** “reject” (* \mathbf{v} is not contained by \mathcal{M}_y^c *)
 - 16: **end if**
-

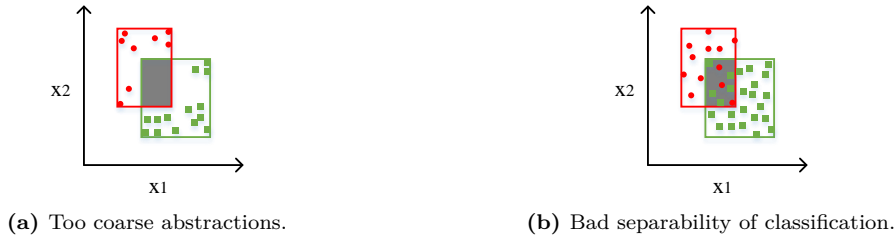


Fig. 4: An illustration of the source of uncertainty.

After constructing the monitor, it will be deployed with the network in parallel and work according to the procedure presented in Algorithm 3. Note that for simplicity in line 4 and 7, we use $\mathbf{v} \in \mathcal{M}_{y,\ell}^c$ ($\mathcal{M}_{y,\ell}^{\text{inc}}$) to denote a vector \mathbf{v} is contained in some element of set $\mathcal{M}_{y,\ell}^c$ ($\mathcal{M}_{y,\ell}^{\text{inc}}$). For each new input, the value at monitored layer ℓ will first be produced (line 2) and then checked (line 4 – 13) whether it is contained by one of abstractions from $\mathcal{M}_{y,\ell}^c$ and $\mathcal{M}_{y,\ell}^{\text{inc}}$ according the network prediction of class y (line 3). Out of the four possibilities, we distinguish three outcomes: i) “uncertainty”, if $f(\mathbf{x})$ is contained by both some abstraction from $\mathcal{M}_{y,\ell}^c$ and $\mathcal{M}_{y,\ell}^{\text{inc}}$; ii) “accept”, if $f(\mathbf{x})$ is only contained by some abstraction from $\mathcal{M}_{y,\ell}^c$; iii) “reject”, otherwise.

Example 6. Consider the network in Fig. 3 and the monitor constructed in Example 5 in parallel. Since there exists no overlap between the built abstractions for each class, the monitor has only two possible outcomes: accept and reject. Assume now $\mathbf{x}^1 = (0.15, 0.1)$ and $\mathbf{x}^2 = (0.6, 0.5)$ are input to the network. We first collect its output at watched layer 2: $f^2(\mathbf{x}^1) = (0.14, 0.13)$, and $f^2(\mathbf{x}^2) = (0.58, 0.56)$. Then, the network outputs the predictions: $\text{dec}(\mathbf{x}^1)=1$, $\text{dec}(\mathbf{x}^2)=1$. Based on the predicted class of each input, the monitor checks if its produced feature is in some corresponding abstractions or not. The determination is that $f^2(\mathbf{x}^1)$ is inside abstraction $A_{1,2}^{C_1}$, while $f^2(\mathbf{x}^2)$ is outside any abstraction in $\mathcal{M}_{1,2}^c$. Finally, the monitor accepts \mathbf{x}^1 and rejects \mathbf{x}^2 .

Remark 3 (About uncertainty). Using “uncertainty” provides a new dimension to verify the quality of the built monitor for a given network, since it measures the “overlap” between the abstractions of correct and incorrect behaviors. The more “uncertainty” a monitor produces as verdict, the worse the abstraction is. The reason for a high level of uncertainty can be twofold, as illustrated in Fig 4: i) the abstraction built is too coarse; ii) the network intrinsically has a bad separability of classification.

5 Experimental Evaluation

The objective of this section is twofold: i) to show that our method for estimating clustering coverage produces precise approximations in practice, i.e., the difference between the estimated lower and upper bounds is zero or negligible; ii) to assess the monitor performance under different settings of clustering parameter τ and chosen monitoring layers.

We use the MNIST [26] benchmark, which is a dataset for image classification of handwritten digits (0 to 9). MNIST consists of a training set of 60,000 samples and a test set of 10,000 samples. We use the test set of F_MNIST [49] to simulate abnormal inputs, that is 10,000 samples from 10 classes of Zalando article images. For consistency, we used the common network in [6] and [19], whose accuracies on training and test sets are 99.76% and 99.24%, respectively. We use the last four layers of the network to build the monitors

(denoted as layer 6, 7, 8, and 9 in what follows). We extract the high-level features from these layers to create the monitors' references. For clustering parameter, we tried out the 12 values in $[1.0, 0.9, 0.8, 0.7, 0.6, 0.5, 0.4, 0.3, 0.2, 0.1, 0.05, 0.01]$. Since a monitor is built for each output class at each monitored layer, 480 monitors in total were constructed and tested during the experimentation.

To reduce the computation cost of the experiments (and facilitate its reproducibility), we divided the experiments in 3 steps:

1. high-level features extraction, which can be one-time generated in seconds and used for multiple times afterwards;
2. partition of the features with many options of clustering parameter, during the experimentation, which took the most time due to the search of the fine k . But, this can be very efficient if the options are tried out in descending order;
3. monitor creation and test, which can be done immediately.

5.1 Clustering Coverage Estimation

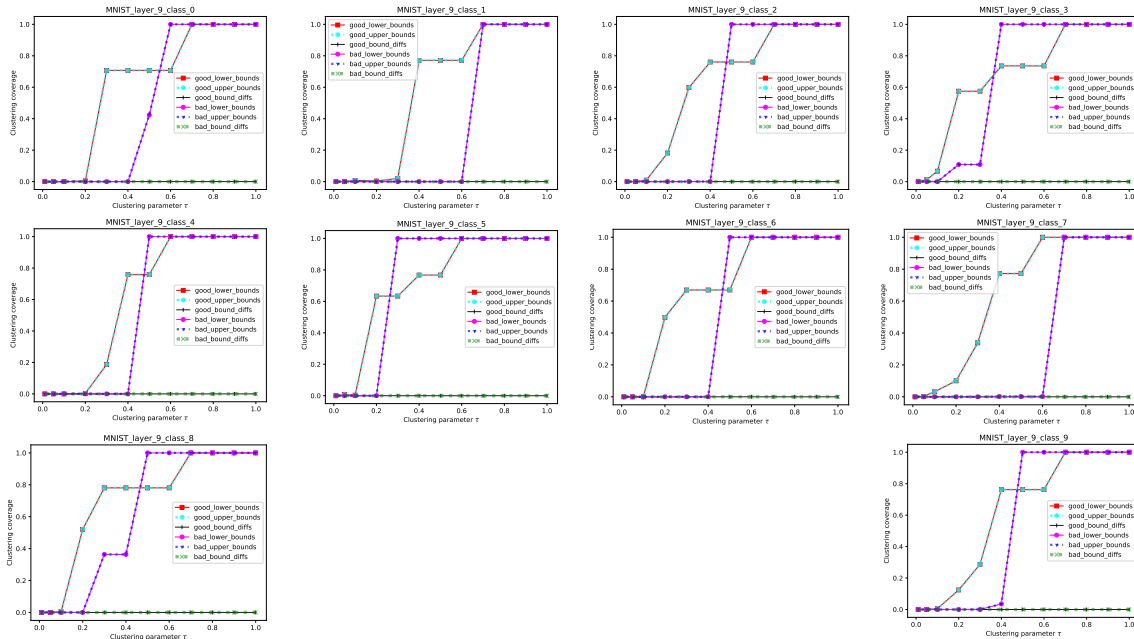


Fig. 5: Clustering coverage estimations for the high-level features obtained at the output layer for benchmark MNIST.

Fig. 5 contains 10 graphs which result from the clustering coverage estimation for partitioning the high-level features at the output layer by using the following clustering parameters $[1.0, 0.9, 0.8, 0.7, 0.6, 0.5, 0.4, 0.3, 0.2, 0.1, 0.05, 0.01]$. Each graph contains six curves which represent the lower bounds, the upper bounds, the bound differences of clustering coverage for the partitions corresponding to the good and bad features used to construct the corresponding monitor reference.

We observed that the relative difference between estimated lower and upper bounds are zeros or extremely small – less than 1%, as shown in Fig. 5. Moreover, as we stated in previous section, the clustering coverage lines close to two endpoint are flat, which indicates that the difference of clustering coverage between the parameters τ in such regions is zero or very small.

Table 2: Confusion matrix giving the different outcomes when evaluating the verdict of a monitor according a network input.

	verdicts	negative (accept)	positive (reject)	uncertainty
real nature				
negative (labelled y)		true negative (TN)	false positive (FP)	missed negative (MN)
positive (labelled non- y)		false negative (FN)	true positive (TP)	missed positive (MP)

5.2 Assessing Monitor Precision

We discuss first how to evaluate the precision of a monitor for a classification system and then the relationship between the performance, the clustering parameter, and the monitored layer.

Evaluating monitors for classification systems. Since we create monitors for image classification systems, we use two sorts of images to construct the test dataset. The first sort is referred to as known inputs; these are the images belonging to one of classes of the system (i.e., from MNIST). The second sort is referred to as unknown inputs; these are the images not belonging to any class of the system (i.e., from F_MNIST). In testing a monitor, one can choose the ratio between known and unknown inputs depending on the criticality and the purpose of the classification system. We choose to have the same number of known and unknown inputs, i.e., we took 10,000 samples from each dataset. Once the test data is prepared, we feed it to the network and evaluate the performance of every monitor by considering different kinds of outcomes as indicated in the confusion matrix shown in Table 2. We note that a false negative can correspond to two situations: a known input from a different class or an unknown input.

Comparison with [19]. Controlling the coarseness of built abstractions with regard to effectiveness is crucial. However, how to control the size of sub-box abstractions via clustering parameter is ignored in [19]. This paper addresses it as follows. First, we introduce the notion of clustering coverage to measure, in terms of covered space, the relative size of sub-box abstractions w.r.t the global one. Second, we leverage the network bad behaviours, which introduces a new monitor outcome of uncertainty. The number of uncertainty outcomes (MN and MP in Table 2) is an hint on the coarseness of built abstractions. Furthermore, we provide the following improvements: 1) the object of study, novelty detection, is refined to each output class of a given network, since the original definition of novelty, *true positive* in [19], includes not only unknown inputs, but also known inputs which belong to one of output classes but misclassified and whose feature is outside abstraction; 2) we use a clustering parameter that is specific to each output class at each monitored layer, and possibly to each set of good and bad features; while [19] uses a uniform clustering parameter for all output classes and monitored layers. This enables precise control on the numbers of FN and FP, e.g., see Fig. 6: a higher F1 score can be always achieved via selecting a group of clustering parameters customized to each output class.

In the sequel, we discuss in details three topics: i) relationship between monitor effectiveness and clustering parameter; ii) how to tune the clustering parameter; iii) how to select the best layers to monitor.

Monitor effectiveness vs clustering parameter. In this experiment, we evaluate the effectiveness of the monitor according to different values of the clustering parameter τ .

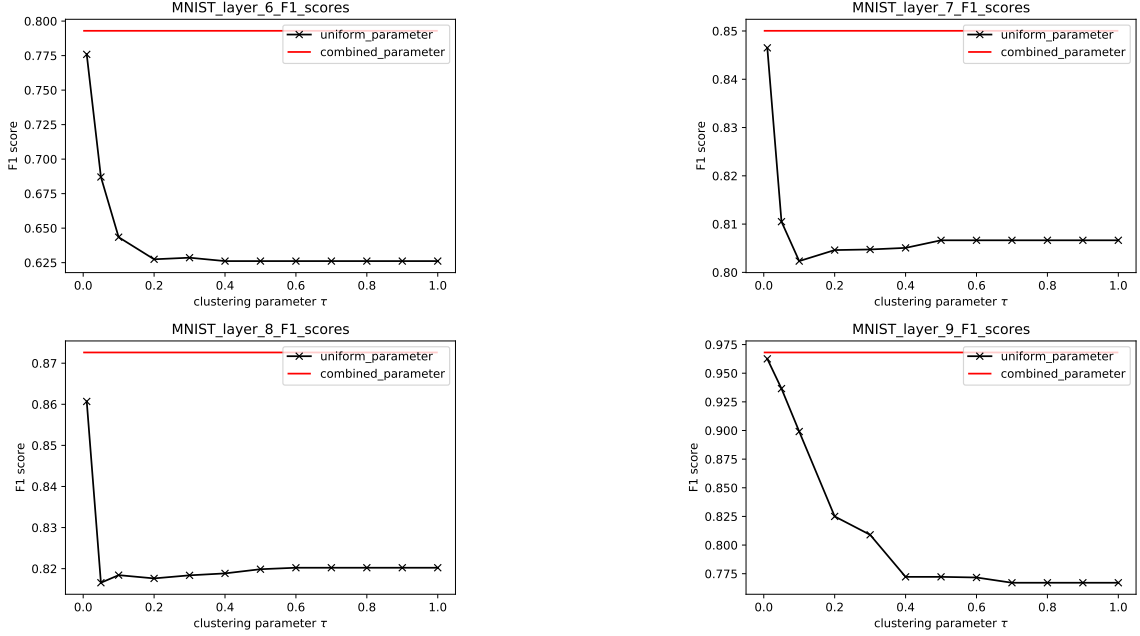


Fig. 6: Comparison of F1 scores obtained via setting uniform (as in [19]) and combined parameters on benchmark MNIST.

Due to space limitation, in Fig. 7, we only present the results of 120 out of 480 monitors, representing 12 configurations of the clustering parameter for each of the 10 output classes. Monitors watch the last layer of the network. Each graph contains a curve depicting the number of occurrences for each of the six possible outcomes defined in Table 2 and the number of real positive and negative samples, according to the values of the clustering parameter. As can be seen, by changing the value of the clustering parameter, one can directly control the sensitivity of the monitor to report an abnormal input. This supports both the proposal of clustering the high-level features into smaller clusters before computing a global abstraction for them and also the idea of selecting a clustering parameter specific for each output-class monitor.

Observing the graphs more closely, we can make the following observations.

1. The number of TN is only affected when the value of τ is very small, in most cases less than 0.1. Consequently, the abstractions for good high-level features are too coarse in most cases.
2. In most cases, the number of uncertainties is zero or reduced to zero by setting a small value of τ . This indicates that our used network has a good separability of classification and also that the abstractions for good and bad features are precise enough. However, we note that the capability of reducing uncertainty to zero may stem from over-precise abstractions, i.e., a feature cluster containing only one feature making the abstractions pointless.
3. In terms of errors of the monitors, the number of FP is very small, meaning that the probability of mis-classifying negative samples is very low, while the number of FN is very high. However, the number of FN can be greatly reduced. This indicates that the detection of positive samples is not good enough due to the coarseness of abstraction.
4. The number of TP can be always augmented by shrinking the abstraction.
5. The monitors for different output classes have different degrees of sensitivity to parameter τ . For example, the performance of monitors for classes 3, 5, 6, and 9 does not depend on the value of τ .

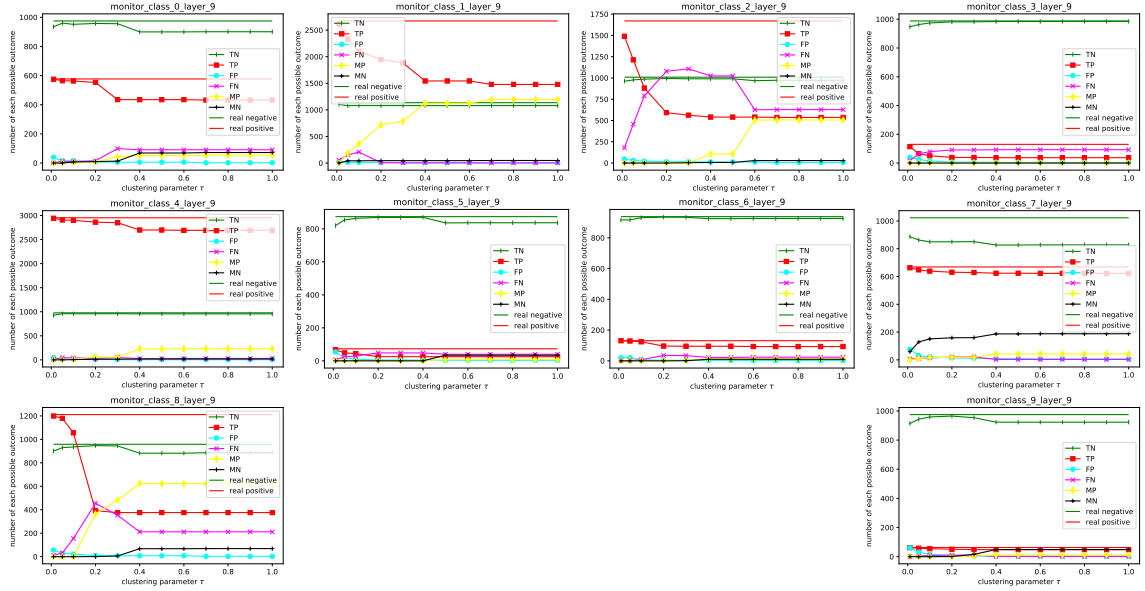


Fig. 7: The numbers of different outcomes in Table 2 for 10 monitors built at the output layer for benchmark MNIST.

Clustering parameter tuning. Clearly, the monitor effectiveness depends the clustering parameter. One can adjust parameter τ to improve the monitor detection capability of positive samples, i.e., abnormal inputs. When adjusting τ , one can observe the following elements: i) the clustering coverage estimation to decide whether the “white space” has been sufficiently removed; ii) the numbers of uncertainties (MN and MP in Table 2) to determine if they can be reduced into zeros, which determines whether the good and bad features can be well separated by box abstractions; iii) the number changes of TN and TP when τ is decreased after reducing the numbers of uncertainties into zeros (i.e., abstractions for good and bad features have been non-overlapping). For instance, if one observes that the number of TN decreases while the number of TP increases in this case, it means that the box abstractions are not able to distinguish the real negative and positive samples. This can be a signal to investigate the appropriateness of the box shape to abstract the features or the network separability, since there exists some region where real negative and positives samples are entangled. Furthermore, the sensitivity of the dependence to the clustering parameter differs among output classes, so it is desirable to fine-tune the clustering parameter for each class separately. This also applies to the monitors built in different layers because the features used to construct a monitor are totally different.

Monitor precision vs monitored layer. We use precision and recall to study the relationship between the monitor effectiveness and the monitored layer. We represent precision-recall curves which show the tradeoff between precision and recall for different values of the clustering parameter τ . *Precision or positive predictive value (PPV)* is defined as the number of TP over the total number of predictive positive samples, i.e., $precision = \frac{TP}{TP+FP}$, while *recall or true positive rate (TPR)* is defined as the number of TP over the total number of real positive samples, i.e., $recall = \frac{TP}{TP+FN+MP}$. A large area under the curve indicates both a high recall and high precision. High precision indicates a low false positive rate, and high recall indicates a low false negative rate. High scores for both show that the classifier is returning accurate results (high precision), as well as returning a majority of all positive results (high recall). Based on this, by examining the precision-recall curves shown in Fig. 8, we can see that for benchmark MNIST, it is better to monitor the output layer, as one can achieve high precision and recall in most cases.

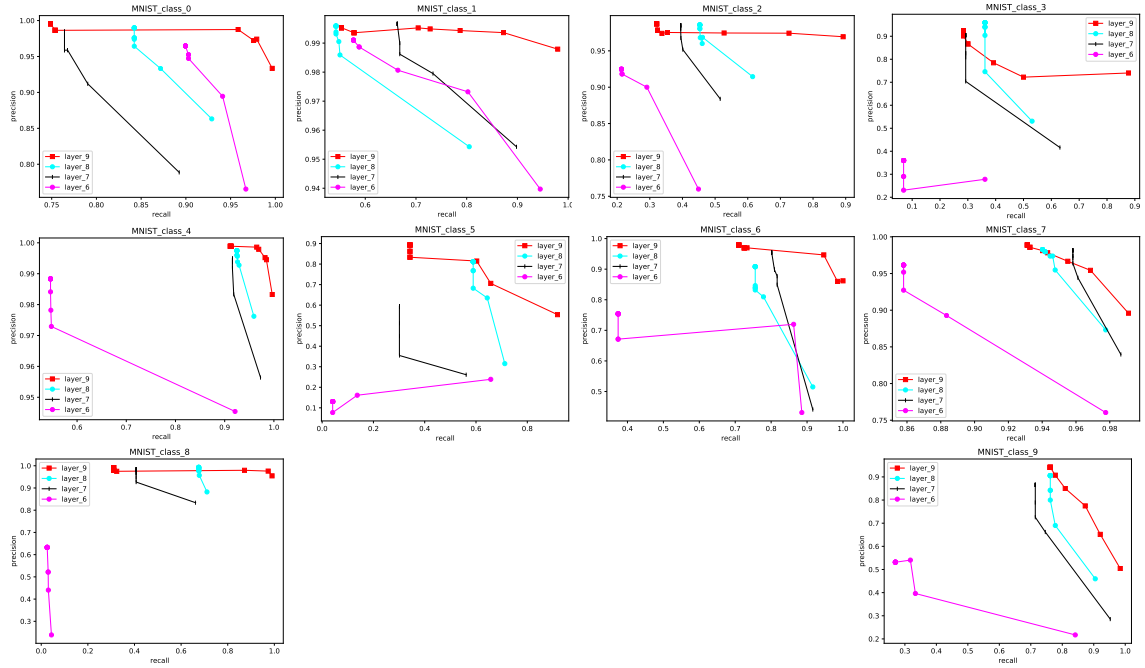


Fig. 8: Precision-Recall curves for monitors built on benchmark MNIST.

5.3 Discussion and Lessons Learned

Our experiments were conducted on a Windows PC (Intel(R) Core(TM) i7-7600U CPU @2.80 GHz, with 8 GB RAM) and the implementation is available ⁵. The construction and test of 480 monitors on benchmark MNIST took, respectively, 2, 473 and 85 seconds. Apart from MNIST, we have also tried out the same experiments on F_MNIST and CIFAR10 [25] and report the results in the appendix.

Thanks to the overall results on different benchmarks, we are more convinced that it is necessary to partition (e.g., clustering here) the high-level used features before computing a global abstraction for them, since on all tried benchmarks there exist many uncertainties (missed positives and negatives). These uncertainties are due to the overlapping between the abstractions built from the good and bad features when these features are not well partitioned, and can be removed when well partitioned, e.g., tuning the clustering parameter into a small value in this paper. In addition to partitioning the features via the clustering method, we suggest that the clustering parameter should be customized for each output-class of a network at different layers, even for the good and bad features used to construct a monitor for same output-class.

However, we point out that the optimal monitored layer is not always the output layer, since we observed on benchmark F_MNIST that in most cases the monitor’s performance at the fourth to the last layer is superior than that ones at the last three layers by observing their precision-recall curves in Fig. 9. Until now, no general law can be given to predict such optimal monitored layer and we believe that it makes the method presented in this paper important to best configure monitors for a given classification system.

Last but not least, the success of using abstraction-based monitors for networks relies on three pivotal factors: i) accuracy and separability of classification of the monitored network, which determines the reliability of the system itself and can not be improved by added monitors; ii) sufficiency of data for constructing a monitor, else the abstraction

⁵ https://gricad-gitlab.univ-grenoble-alpes.fr/rvai-public/abstraction_based_monitors

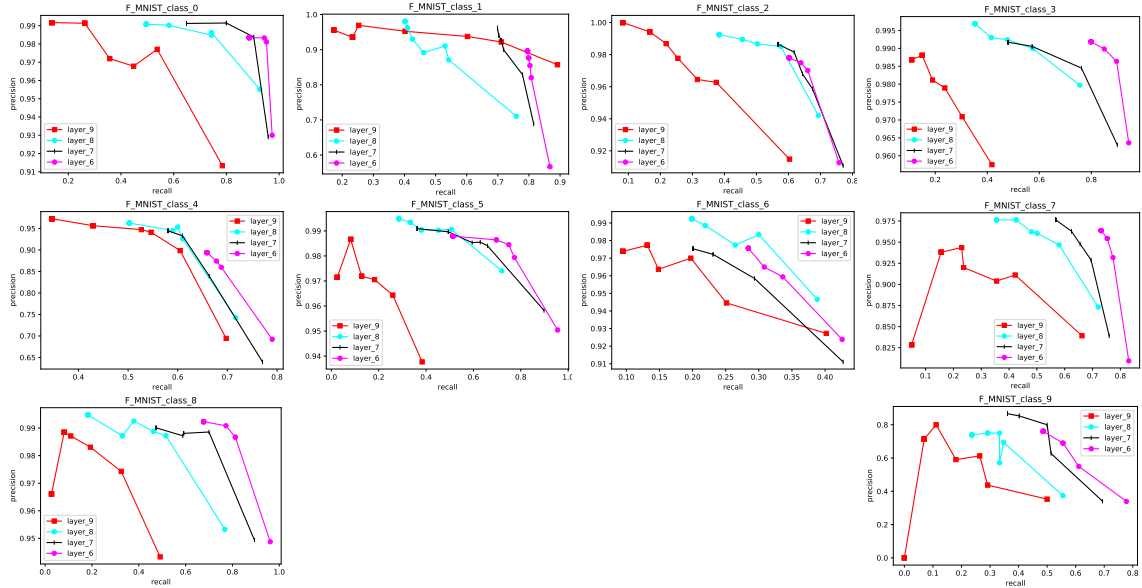


Fig. 9: Precision-Recall curves for monitors built on benchmark F_MNIST.

will be not representative so that the monitor is not reliable; iii) implementation error of network and monitors since the construction and membership query of box abstractions demand precise computation.

6 Related Work

There is a myriad of approaches and formalisms for handling data in runtime verification such as QEA [1], parametric trace slicing [38], see [17] for an overview. However, these approaches essentially consist in augmenting a behavior-based specification formalism such as finite-state machines to handle data rather than verifying a data-oriented system

Hence, in this section, we compare with the approaches aiming at assessing the decisions of neural networks to improve the confidence (in safety-critical scenarios).

One of the first technique for this purpose is anomaly detection, which has been extensively studied in the areas of statistics and traditional machine learning; see [20,4,3] for surveys. All recent anomaly detection approaches [13,15,29,8,23,45] consist essentially in computing a confidence score over the network decisions. Whenever a decision has a score below the required threshold, the decision is rejected and the input declared abnormal. For instance, in the context of deep learning, [18] is a well-known method that calculates a confidence score for the network decision in terms of sample distribution, where the confidence score is the softmax prediction probability of decisions.

The above referred methods are based on a statistical approach. Some more recent work [6,19,5,32], inspired from formal methods, follow the same purposes by building runtime monitors to supervise the decision of a network. Such runtime monitoring approaches fundamentally differ from the traditional runtime verification and monitoring approaches for software and hardware systems (cf. [16,27,11,2]) in that (1) the monitors are not obtained from formal specifications and (2) monitors focus on the data output of the network instead of some property about the ordering of actions. In these approaches, an input into a network is declared as an anomaly when the network decision is rejected by the monitor according to some references. The verdict of a monitor on a new input is based on the membership test of the induced neuron activation pattern in a pre-established sound

over-approximation of neuron activation patterns recorded from network correct decisions constructed from re-applying the training dataset on a well trained network. The approach in [6] uses boolean abstraction to approximate and represent neuron activation patterns from correctly classified training data and is effective on reporting network misclassifications. However, the construction and membership test of boolean formula are computationally expensive, especially when dealing with patterns at layers with many neurons, e.g, running out of 8 GB memory when building such formula for a layer of 84 neurons. To reduce the complexity of abstraction methods, the approach in [19] introduces *box abstraction*, which can be easily computed and membership tested. The paper introduces the idea of partitioning the obtained patterns into smaller clusters first and then constructing abstractions on these smaller clusters. Furthermore, [32] extends [19] by defining a framework of active monitoring of networks based on box abstractions that detects unknown classes of inputs and adapts to them at runtime by virtue of human interactions and retraining the network.

The approach in this paper is in the line of the ones in [6,19] complements the framework of runtime monitors in [6] and [19]. Our approach generalizes these approach by allowing to observe and record the neuron activation patterns at hidden and output layers from both correct and incorrect classifications of known classes of inputs. Additional patterns from misclassified known classes of inputs introduces “uncertainty” verdicts, which provides insights to the precision of the abstraction-based monitor and the separability of network. We extended the idea of applying clustering before constructing abstractions by introducing *boxes with a resolution* which allow defining clustering coverage as a metric to quantify the precision improvement in terms of the spaces covered by the box abstraction constructed with and without clustering. Consequently, one can compare the effectiveness of different clustering parameters and tune the parameter of the monitoring approach.

7 Conclusion and Future Research Directions

We introduce a framework for the runtime monitoring of LECs with forward neural networks. Our framework relies on boxes with resolution which are used to abstract the data seen during training and allows a monitor to state an accept/reject/uncertainty verdict based on the membership test of a new input to the built abstractions. Resolution of boxes allows quantifying the coverage of the abstractions used by monitors and thus assessing their precision. We showed experiments showing how an expert can fine-tune the parameters of the monitoring framework (clustering parameter and watched layers). The notion of uncertainty allows understanding the uncertainty of networks decisions from a formal perspective.

As we believe, we are at the beginning of the search for defining methods and tools for verifying and monitoring learning-enabled components, a lot of research questions and perspectives remain to be addressed. We chose to follow [19,32,5] and build upon the notion of box as such abstraction seems to provide a good tradeoff between precision and performance but a lot of other candidate abstractions (defined in the verification and compilation communities for instance) remain to be studied for monitoring purposes. In terms of monitoring, being able to update at operation time the build abstraction would permit monitors that continuously learn even operation-time inputs. Moreover, the question of reaction to abnormal inputs remains to be studied. More generally, we believe that LECs will need different interacting and complementary methods and toolsets to provide comprehensive solutions affording the needed confidence in the implemented systems, e.g., testing and monitoring for design time, monitoring and enforcement for operation time.

References

1. Barringer, H., Falcone, Y., Havelund, K., Reger, G., Rydeheard, D.E.: Quantified event automata: Towards expressive and efficient runtime monitors. In: Giannakopoulou, D., Méry, D. (eds.) FM 2012: Formal Methods - 18th International Symposium, Paris, France, August 27-31, 2012. Proceedings. Lecture Notes in Computer Science, vol. 7436, pp. 68–84. Springer (2012). https://doi.org/10.1007/978-3-642-32759-9_9
2. Bartocci, E., Falcone, Y. (eds.): Lectures on Runtime Verification - Introductory and Advanced Topics, Lecture Notes in Computer Science, vol. 10457. Springer (2018). <https://doi.org/10.1007/978-3-319-75632-5>
3. Chalapathy, R., Chawla, S.: Deep learning for anomaly detection: A survey. arXiv preprint 1901.03407 (2019)
4. Chandola, V., Banerjee, A., Kumar, V.: Anomaly detection: A survey. ACM computing surveys (CSUR) **41**(3), 1–58 (2009)
5. Cheng, C.H.: Provably-robust runtime monitoring of neuron activation patterns. arXiv preprint 2011.11959 (2020)
6. Cheng, C.H., Nührenberg, G., Yasuoka, H.: Runtime monitoring neuron activation patterns. In: 2019 Design, Automation & Test in Europe Conference & Exhibition (DATE). pp. 300–303. IEEE (2019)
7. Cousot, P., Cousot, R.: Abstract interpretation frameworks. Journal of logic and computation **2**(4), 511–547 (1992)
8. DeVries, T., Taylor, G.W.: Learning confidence for out-of-distribution detection in neural networks. arXiv preprint 1802.04865 (2018)
9. Dutta, S., Jha, S., Sankaranarayanan, S., Tiwari, A.: Output range analysis for deep feedforward neural networks. In: Dutle, A., Muñoz, C.A., Narkawicz, A. (eds.) NASA Formal Methods - 10th International Symposium, NFM 2018, Newport News, VA, USA, April 17-19, 2018, Proceedings. Lecture Notes in Computer Science, vol. 10811, pp. 121–138. Springer (2018). https://doi.org/10.1007/978-3-319-77935-5_9
10. Ehlers, R.: Formal verification of piece-wise linear feed-forward neural networks. In: D’Souza, D., Kumar, K.N. (eds.) Automated Technology for Verification and Analysis - 15th International Symposium, ATVA 2017, Pune, India, October 3-6, 2017, Proceedings. Lecture Notes in Computer Science, vol. 10482, pp. 269–286. Springer (2017). https://doi.org/10.1007/978-3-319-68167-2_19
11. Falcone, Y., Havelund, K., Reger, G.: A tutorial on runtime verification. In: Broy, M., Peled, D.A., Kalus, G. (eds.) Engineering Dependable Software Systems, NATO Science for Peace and Security Series, D: Information and Communication Security, vol. 34, pp. 141–175. IOS Press (2013). <https://doi.org/10.3233/978-1-61499-207-3-141>
12. Gehr, T., Mirman, M., Drachler-Cohen, D., Tsankov, P., Chaudhuri, S., Vechev, M.: Ai2: Safety and robustness certification of neural networks with abstract interpretation. In: 2018 IEEE Symposium on Security and Privacy (SP). pp. 3–18. IEEE (2018)
13. Geifman, Y., El-Yaniv, R.: Selective classification for deep neural networks. arXiv preprint 1705.08500 (2017)
14. Gowal, S., Dvijotham, K., Stanforth, R., Bunel, R., Qin, C., Uesato, J., Arandjelovic, R., Mann, T., Kohli, P.: On the effectiveness of interval bound propagation for training verifiably robust models. arXiv preprint 1810.12715 (2018)
15. Guo, C., Pleiss, G., Sun, Y., Weinberger, K.Q.: On calibration of modern neural networks. In: International Conference on Machine Learning. pp. 1321–1330. PMLR (2017)
16. Havelund, K., Goldberg, A.: Verify your runs. In: Meyer, B., Woodcock, J. (eds.) Verified Software: Theories, Tools, Experiments, First IFIP TC 2/WG 2.3 Conference, VSTTE 2005, Zurich, Switzerland, October 10-13, 2005, Revised Selected Papers and Discussions. Lecture Notes in Computer Science, vol. 4171, pp. 374–383. Springer (2005). https://doi.org/10.1007/978-3-540-69149-5_40
17. Havelund, K., Reger, G., Thoma, D., Zalinescu, E.: Monitoring events that carry data. In: Bartocci, E., Falcone, Y. (eds.) Lectures on Runtime Verification - Introductory and Advanced Topics, Lecture Notes in Computer Science, vol. 10457, pp. 61–102. Springer (2018). https://doi.org/10.1007/978-3-319-75632-5_3
18. Hendrycks, D., Gimpel, K.: A baseline for detecting misclassified and out-of-distribution examples in neural networks. arXiv preprint 1610.02136 (2016)
19. Henzinger, T.A., Lukina, A., Schilling, C.: Outside the box: Abstraction-based monitoring of neural networks. arXiv preprint arXiv:1911.09032 (2019)
20. Hodge, V., Austin, J.: A survey of outlier detection methodologies. Artificial intelligence review **22**(2), 85–126 (2004)
21. Huang, X., Kwiatkowska, M., Wang, S., Wu, M.: Safety verification of deep neural networks. In: Majumdar, R., Kunčak, V. (eds.) Computer Aided Verification - 29th International Conference, CAV 2017, Heidelberg, Germany, July 24-28, 2017, Proceedings, Part I. Lecture Notes in Computer Science, vol. 10426, pp. 3–29. Springer (2017). https://doi.org/10.1007/978-3-319-63387-9_1
22. Intelligence, F.C.F.A.: Research challenge ii: Dependability, finnish center for artificial intelligence (2018)

23. Jiang, H., Kim, B., Guan, M.Y., Gupta, M.R.: To trust or not to trust a classifier. In: NeurIPS. pp. 5546–5557 (2018)
24. Katz, G., Barrett, C.W., Dill, D.L., Julian, K., Kochenderfer, M.J.: Reluplex: An efficient SMT solver for verifying deep neural networks. In: Majumdar, R., Kuncak, V. (eds.) Computer Aided Verification - 29th International Conference, CAV 2017, Heidelberg, Germany, July 24–28, 2017, Proceedings, Part I. Lecture Notes in Computer Science, vol. 10426, pp. 97–117. Springer (2017). https://doi.org/10.1007/978-3-319-63387-9_5
25. Krizhevsky, A., Hinton, G., et al.: Learning multiple layers of features from tiny images (2009)
26. LeCun, Y., Bottou, L., Bengio, Y., Haffner, P.: Gradient-based learning applied to document recognition. *Proceedings of the IEEE* **86**(11), 2278–2324 (1998)
27. Leucker, M., Schallhart, C.: A brief account of runtime verification. *J. Log. Algebraic Methods Program.* **78**(5), 293–303 (2009). <https://doi.org/10.1016/j.jlap.2008.08.004>
28. Li, J., Liu, J., Yang, P., Chen, L., Huang, X., Zhang, L.: Analyzing deep neural networks with symbolic propagation: Towards higher precision and faster verification. In: Chang, B.E. (ed.) Static Analysis - 26th International Symposium, SAS 2019, Porto, Portugal, October 8–11, 2019, Proceedings. Lecture Notes in Computer Science, vol. 11822, pp. 296–319. Springer (2019). https://doi.org/10.1007/978-3-030-32304-2_15
29. Liang, S., Li, Y., Srikant, R.: Enhancing the reliability of out-of-distribution image detection in neural networks. arXiv preprint 1706.02690 (2017)
30. Lloyd, S.: Least squares quantization in pcm. *IEEE transactions on information theory* **28**(2), 129–137 (1982)
31. Lomuscio, A., Maganti, L.: An approach to reachability analysis for feed-forward relu neural networks. *CoRR* **abs/1706.07351** (2017)
32. Lukina, A., Schilling, C., Henzinger, T.A.: Into the unknown: Active monitoring of neural networks. arXiv preprint 2009.06429 (2020)
33. Murtagh, F., Contreras, P.: Algorithms for hierarchical clustering: an overview. *Wiley Interdisciplinary Reviews: Data Mining and Knowledge Discovery* **2**(1), 86–97 (2012)
34. Narodytska, N., Kasiviswanathan, S.P., Ryzhyk, L., Sagiv, M., Walsh, T.: Verifying properties of binarized deep neural networks. In: McIlraith, S.A., Weinberger, K.Q. (eds.) Proceedings of the Thirty-Second AAAI Conference on Artificial Intelligence, (AAAI-18), the 30th innovative Applications of Artificial Intelligence (IAAI-18), and the 8th AAAI Symposium on Educational Advances in Artificial Intelligence (EAAI-18), New Orleans, Louisiana, USA, February 2–7, 2018. pp. 6615–6624. AAAI Press (2018)
35. Neema, S.: Assured autonomy
36. Pei, K., Cao, Y., Yang, J., Jana, S.: Deepxplore: Automated whitebox testing of deep learning systems. In: proceedings of the 26th Symposium on Operating Systems Principles. pp. 1–18 (2017)
37. Pulina, L., Tacchella, A.: An abstraction-refinement approach to verification of artificial neural networks. In: Touili, T., Cook, B., Jackson, P.B. (eds.) Computer Aided Verification, 22nd International Conference, CAV 2010, Edinburgh, UK, July 15–19, 2010. Proceedings. Lecture Notes in Computer Science, vol. 6174, pp. 243–257. Springer (2010). https://doi.org/10.1007/978-3-642-14295-6_24
38. Rosu, G., Chen, F.: Semantics and algorithms for parametric monitoring. *Log. Methods Comput. Sci.* **8**(1) (2012). [https://doi.org/10.2168/LMCS-8\(1:9\)2012](https://doi.org/10.2168/LMCS-8(1:9)2012), [https://doi.org/10.2168/LMCS-8\(1:9\)2012](https://doi.org/10.2168/LMCS-8(1:9)2012)
39. Ruan, W., Huang, X., Kwiatkowska, M.: Reachability analysis of deep neural networks with provable guarantees. In: Lang, J. (ed.) Proceedings of the Twenty-Seventh International Joint Conference on Artificial Intelligence, IJCAI 2018, July 13–19, 2018, Stockholm, Sweden. pp. 2651–2659. ijcai.org (2018). <https://doi.org/10.24963/ijcai.2018/368>
40. Schubert, E., Sander, J., Ester, M., Kriegel, H.P., Xu, X.: Dbscan revisited, revisited: why and how you should (still) use dbscan. *ACM Transactions on Database Systems (TODS)* **42**(3), 1–21 (2017)
41. Sculley, D., Holt, G., Golovin, D., Davydov, E., Phillips, T., Ebner, D., Chaudhary, V., Young, M., Crespo, J., Dennison, D.: Hidden technical debt in machine learning systems. In: Cortes, C., Lawrence, N.D., Lee, D.D., Sugiyama, M., Garnett, R. (eds.) Advances in Neural Information Processing Systems 28: Annual Conference on Neural Information Processing Systems 2015, December 7–12, 2015, Montreal, Quebec, Canada. pp. 2503–2511 (2015)
42. Seshia, S.A., Sadigh, D.: Towards verified artificial intelligence. *CoRR* **abs/1606.08514** (2016)
43. Sun, Y., Huang, X., Kroening, D., Sharp, J., Hill, M., Ashmore, R.: Testing deep neural networks. arXiv preprint 1803.04792 (2018)
44. Szegedy, C., Zaremba, W., Sutskever, I., Bruna, J., Erhan, D., Goodfellow, I.J., Fergus, R.: Intriguing properties of neural networks. In: Bengio, Y., LeCun, Y. (eds.) 2nd International Conference on Learning Representations, ICLR 2014, Banff, AB, Canada, April 14–16, 2014, Conference Track Proceedings (2014)
45. Thulasidasan, S., Bhattacharya, T., Bilmes, J., Chennupati, G., Mohd-Yusof, J.: Combating label noise in deep learning using abstention. arXiv preprint 1905.10964 (2019)
46. Tian, Y., Pei, K., Jana, S., Ray, B.: Deeptest: Automated testing of deep-neural-network-driven autonomous cars. In: Proceedings of the 40th international conference on software engineering. pp. 303–314 (2018)

47. Weng, T., Zhang, H., Chen, H., Song, Z., Hsieh, C., Daniel, L., Boning, D.S., Dhillon, I.S.: Towards fast computation of certified robustness for relu networks. In: Dy, J.G., Krause, A. (eds.) Proceedings of the 35th International Conference on Machine Learning, ICML 2018, Stockholmsmässan, Stockholm, Sweden, July 10-15, 2018. Proceedings of Machine Learning Research, vol. 80, pp. 5273–5282. PMLR (2018)
48. Wicker, M., Huang, X., Kwiatkowska, M.: Feature-guided black-box safety testing of deep neural networks. In: International Conference on Tools and Algorithms for the Construction and Analysis of Systems. pp. 408–426. Springer (2018)
49. Xiao, H., Rasul, K., Vollgraf, R.: Fashion-mnist: a novel image dataset for benchmarking machine learning algorithms. arXiv preprint 1708.07747 (2017)
50. Xie, X., Ma, L., Juefei-Xu, F., Chen, H., Xue, M., Li, B., Liu, Y., Zhao, J., Yin, J., See, S.: Coverage-guided fuzzing for deep neural networks. arXiv preprint 1809.01266 **3** (2018)

A Additional Experimental Results on Benchmarks F_MNIST and CIFAR10

We present the results referred to in the experimental section related to clustering coverage estimation, numbers of outcomes as per Table 2, and precision-recall curves obtained on benchmark F_MNIST and CIFAR10.

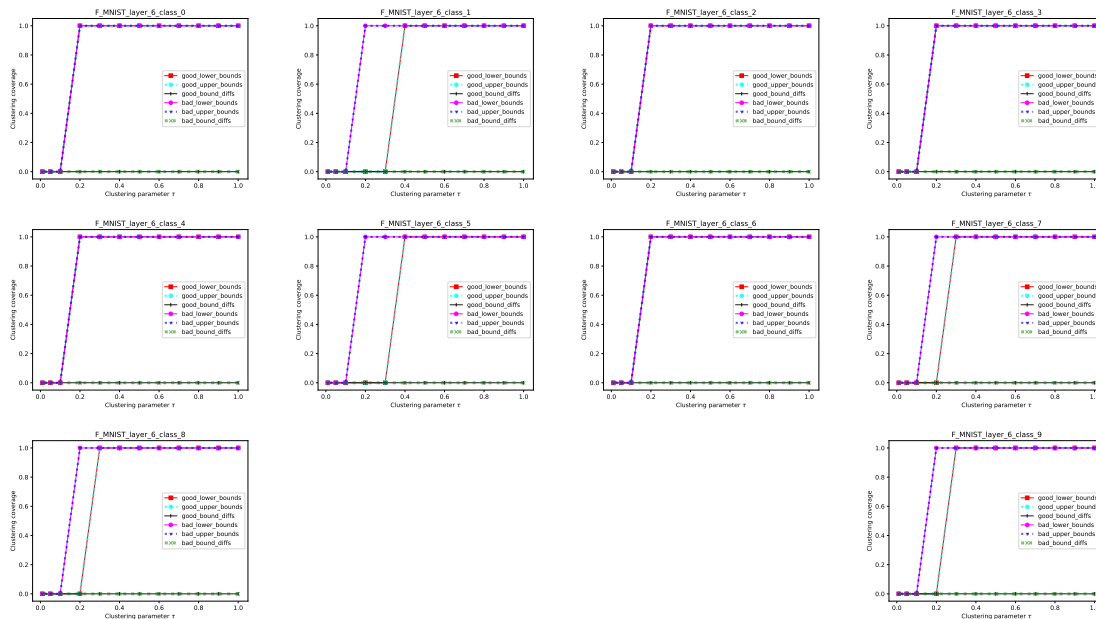


Fig. 10: Clustering coverage estimations for the high-level features obtained at the output layer for benchmark F_MNIST.

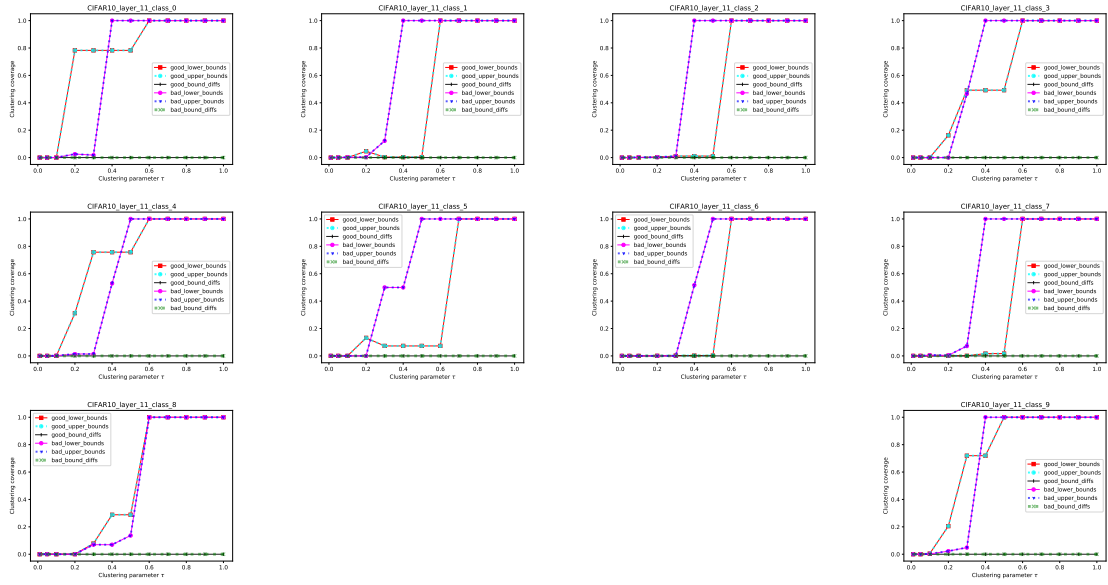


Fig. 11: Clustering coverage estimations for the high-level features obtained at the output layer for benchmark CIFAR10.

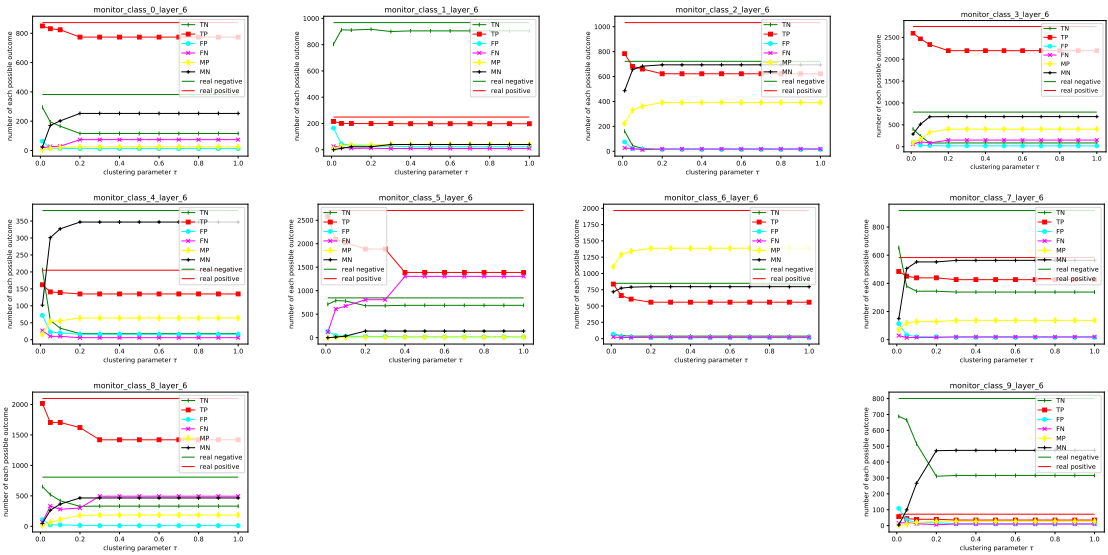


Fig. 12: The numbers of different outcomes in Table 2 for 10 monitors built at layer 6 for benchmark F_MNIST.

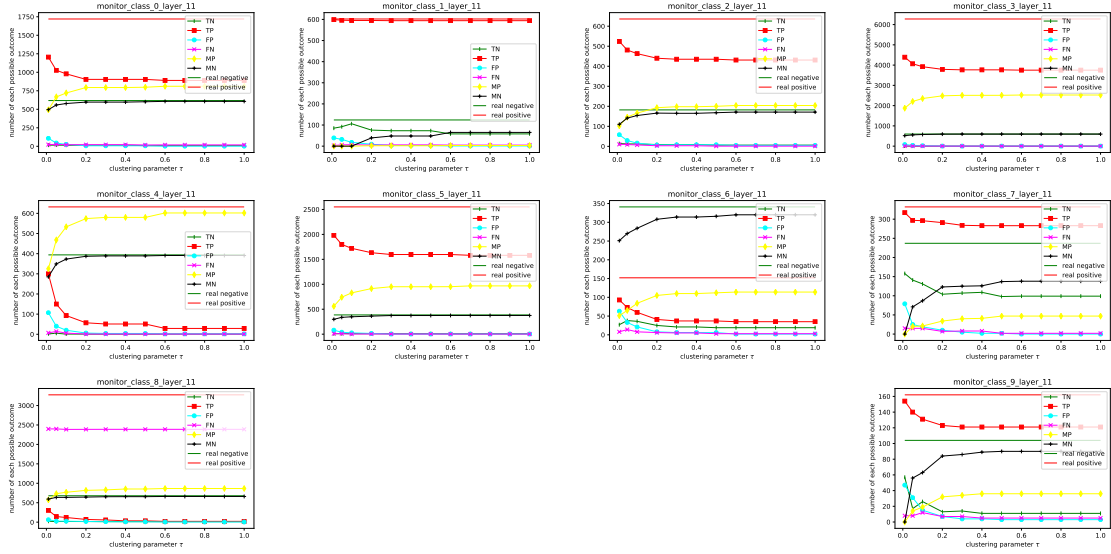


Fig. 13: The numbers of different outcomes in Table 2 for 10 monitors built at the output layer for benchmark CIFAR10.

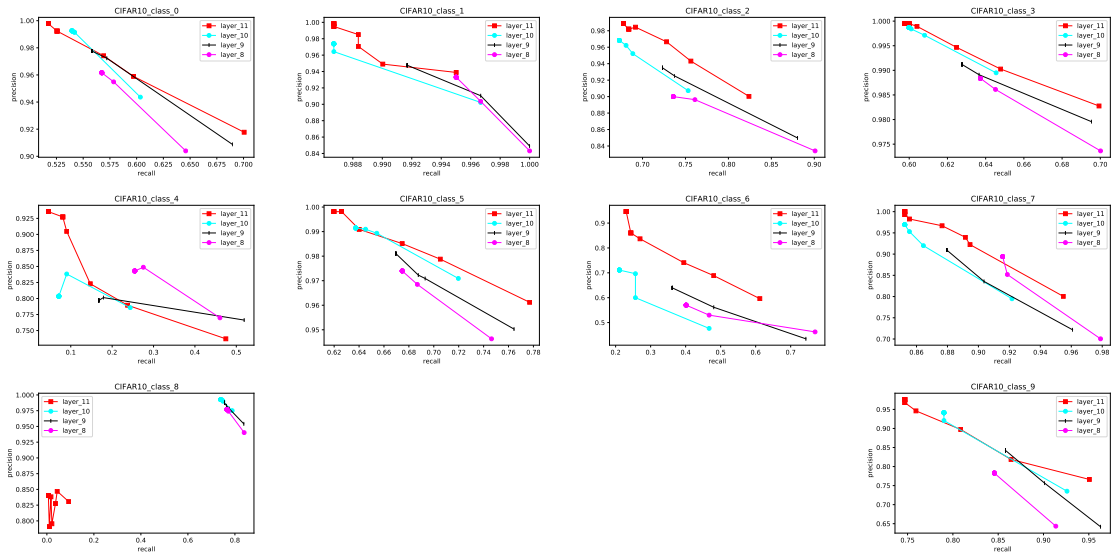


Fig. 14: Precision-recall curves for monitors built on benchmark CIFAR10.